Cerebral Cortex, September 2020;30: 4747–4758

doi: 10.1093/cercor/bhaa032
Advance Access Publication Date: 30 March 2020
Original Article

ORIGINAL ARTICLE

Prism Adaptation Modulates Connectivity of the Intraparietal Sulcus with Multiple Brain Networks

Selene Schintu[1,2], Michael Freedberg[1], Stephen J. Gotts[3], Catherine A. Cunningham[1], Zaynah M. Alam[1], Sarah Shomstein[2] and Eric M. Wassermann[1]

[1]Behavioral Neurology Unit, National Institute of Neurological Disorders and Stroke Bethesda, MD 20892, USA, [2]Department of Psychology George Washington University Washington, DC 20052, USA and [3]Laboratory of Brain and Cognition, National Institute of Mental Health, Bethesda, MD 20892, USA

Address correspondence to Selene Schintu, Behavioral Neurology Unit, National Institute of Neurological Disorders and Stroke, Building 10, Room 7D48, 10 Center Drive, MSC 1440, Bethesda, MD 20892-1430, USA. Email: selene.schintu@gmail.com

Abstract

Prism adaptation (PA) alters spatial cognition according to the direction of visual displacement by temporarily modifying sensorimotor mapping. Right-shifting prisms (right PA) improve neglect of left visual field in patients, possibly by decreasing activity in the left hemisphere and increasing it in the right. Left PA shifts attention rightward in healthy individuals by an opposite mechanism. However, functional imaging studies of PA are inconsistent, perhaps because of differing activation tasks. We measured resting-state functional connectivity (RSFC) in healthy individuals before and after PA. When contrasted, right versus left PA decreased RSFC in the spatial navigation network defined by the right posterior parietal cortex (PPC), hippocampus, and cerebellum. Within-PA-direction comparisons showed that right PA increased RSFC in subregions of the PPCs and between the PPCs and the right middle frontal gyrus and left PA decreased RSFC between these regions. Both right and left PA decreased RSFC between the PPCs and bilateral temporal areas. In summary, right PA increases connectivity in the right frontoparietal network and left PA produces essentially opposite effects. Furthermore, right, compared with left, PA modulates RSFC in the right hemisphere navigation network.

Key words: navigation network, neglect, parahippocampal gyrus, parietal cortex, visuospatial attention

Introduction

Adaptation to prisms, which shift vision laterally, temporarily modifies sensorimotor mapping (Helmholtz 1867; Rossetti et al. 1998). Prism adaptation (PA) is performed by practicing pointing movements to a displaced target, resulting in a rapid correction of the pointing error and a corresponding aftereffect in the opposite direction after the prisms are removed. Those aftereffects are not limited to the sensorimotor domain, but also affect cognition (Rossetti et al. 1998).

Adaptation to right-shifting prisms (right PA) biases attention to the left and is a promising technique for improving visuospatial neglect after right hemisphere damage (Rossetti et al. 1998; Azouvi et al. 2017). Right PA in neglect patients ameliorates not only visual abnormalities, such as the rightward shift in line bisection performance but also extinction of tactile and auditory stimuli on the left, altered perception of time (for a review see Clarke and Crottaz-Herbette 2016), and impaired mental time traveling (Anelli and Frassinetti 2019). Left PA produces neglect-like behavior in healthy individuals (Colent et al. 2000; Schintu et al. 2014) by decreasing the inherent leftward bias (pseudoneglect; Bowers and Heilman 1980) and affects not only visuospatial cognition, but also spatial remapping, perception of time (for a review see Michel 2016), and feedback-learning performance (Schintu et al. 2018).

There is general agreement regarding the behavioral consequences of PA. However, the underlying neural changes are not clear and the results of the few studies investigating them are inconsistent. Functional imaging studies of PA have implicated the cerebellum (Weiner et al. 1983; Küper et al. 2014; Werner et al. 2014) and posterior parietal areas during both adaptation (Clower et al. 1996; Luauté et al. 2009; Chapman et al. 2010) and the aftereffect phase (Crottaz-Herbette et al. 2014; Magnani et al. 2014; Schintu et al. 2016). There is also evidence that the PA effect is mediated by the dorsal frontoparietal network (Striemer and Danckert 2010; Saj et al. 2013; Magnani et al. 2014; Schintu et al. 2016), which controls visually guided motor behavior and visual attention (Corbetta and Shulman 2002; Milner and Goodale 2006). However, while some studies have found only frontoparietal network involvement (Saj et al. 2013), others (Luaute et al. 2006; Crottaz-Herbette et al. 2017; Tissieres et al. 2018) describe changes extending to the ventral attentional network in the temporal lobe and modulation of coupling between the attentional and default mode networks (Wilf et al. 2019). Whether PA affects both the dorsal and ventral networks is still unknown. Another open question is whether the PA-induced changes are bilateral or unilateral, and, if bilateral, whether the direction of change in function is the same in both hemispheres. According to an influential model (Pisella et al. 2006; Striemer and Danckert 2010), PA has an opposite mechanism of action according to the direction of the visual displacement: right PA induces its leftward attentional shift in neglect patients by decreasing activity in the intact left hemisphere and increasing it in the right, whereas left PA causes rightward bias in healthy individuals by doing the opposite. A few studies (Luaute et al. 2006; Crottaz-Herbette et al. 2014, 2017) support this model, but others favor a unilateral (Tsujimoto et al. 2018) or a bilateral and unidirectional (Saj et al. 2013) effect.

One reason for the inconsistencies in the literature could be that most functional imaging studies of PA have employed event-related designs and measured local changes in activity. Task-related activation changes may fail to identify brain areas whose connectivity is affected by PA but are not activated by the task. The task itself may also alter the state of the visual attention system in ways which obscure the effects of PA. Resting-state functional connectivity (RSFC) measures dynamic changes in connectivity within networks without depending on task-related activation. In the one existing study of RSFC changes following PA (Tsujimoto et al. 2018), right PA modulated RSFC in the right dorsal network. However, the analysis was limited to regions of interest in the dorsal and ventral networks and may have failed to reveal changes in other brain areas. Investigating the effect of PA on RSFC across the entire brain, without choosing networks *a priori*, is a more rigorous test of mechanistic hypotheses and may reveal previously hidden aspects of the PA mechanism, helping to reconcile conflicting results in the literature.

The aim of this study was to investigate the effect of PA at the whole brain level by comparing the effects of left and right PA on RSFC in healthy subjects. Based on the prevailing PA model (Pisella et al. 2006; Striemer and Danckert 2010), we hypothesized that PA should differentially change behavior and RSFC according to the direction of the visual displacement: right PA should produce a leftward behavioral bias in association with decreasing RSFC in the left frontoparietal network and increasing RSFC in the right, whereas left PA should induce a rightward behavioral bias with opposite connectivity changes.

Materials and Methods

Participants

Forty adults, free of neurological disorders or medications affecting brain function, participated in the study. All had normal or corrected-to-normal vision, were right handed (Edinburgh Inventory; Oldfield 1971), and were right-eye dominant (hole-in-card test; Miles 1930). Participants were compensated for participation and gave written informed consent. The study was approved by the National Institutes of Health, Central Nervous System Institutional Review Board, and conducted in accordance with the ethical standards of the 1964 Declaration of Helsinki (World Medical Association 2013).

Twenty participants (12 female; age = 26.25 ± 0.87 SEM) underwent left PA and the other twenty (13 female; age = 26.12 ± 1.05 SEM) right PA. After data collection, two participants were excluded from the right PA group, one because of excessive motion during scans (average motion > 0.2 cm) and one because of a congenital cerebral cyst, which might have been associated with cortical reorganization. The data submitted to the statistical analysis were gathered from a total of 38 participants: left PA group (12 female; age = 26.25 ± 0.87 SEM) and right PA group (12 female; age = 25.73 ± 1.09 SEM). The left and right PA groups did not differ in age ($t(36) = 0.375$, $P = 0.710$).

Procedures

The experiment consisted of two sessions of behavioral testing and fMRI, one before and one after PA (Fig. 1). In each session, we measured visuospatial performance with the perceptual line bisection and manual line bisection tasks. Then, participants underwent neuroimaging consisting of resting state scans (two runs of 5 minutes) and population receptive field scans (30 minutes; to be reported elsewhere). Following the resting state and population receptive field scans, we repeated the perceptual line bisection and manual line bisection tasks, along with two tasks assessing proprioceptive (straight-ahead pointing) and sensorimotor (open-loop pointing) performance (Fig. 1). Participants then underwent left or right PA. Immediately after PA (early postadaptation assessment), we assessed proprioceptive and sensorimotor performance with the straight-ahead and open-loop pointing tasks and performed another resting state and pRF scan, followed by the perceptual and manual line bisection and the straight-ahead and open-loop pointing tasks (late postadaptation assessment).

During the behavioral measures and PA, participants were seated in front of a horizontal board with their heads supported by a chinrest. On the board, three circular targets (8 mm in diameter) were positioned at 0, −10 (left), and + 10 (right), degrees from the body midline, approximately 57 cm from participant's nasion and were used for the postadaptation, open-loop, and straight-ahead pointing tasks.

Prism Adaptation

During PA, participants were fitted with prism goggles with a 15° left (left PA) or right (right PA) visual field deviation and performed 150 pointing movements to the right and left targets in a verbally cued, pseudorandom, order. Before each pointing movement, participants placed their right index finger in the starting position on a 1.5-cm diameter pad, located close to the midline of the chest. Participants could not see their hands in the starting position and during the first third of the pointing

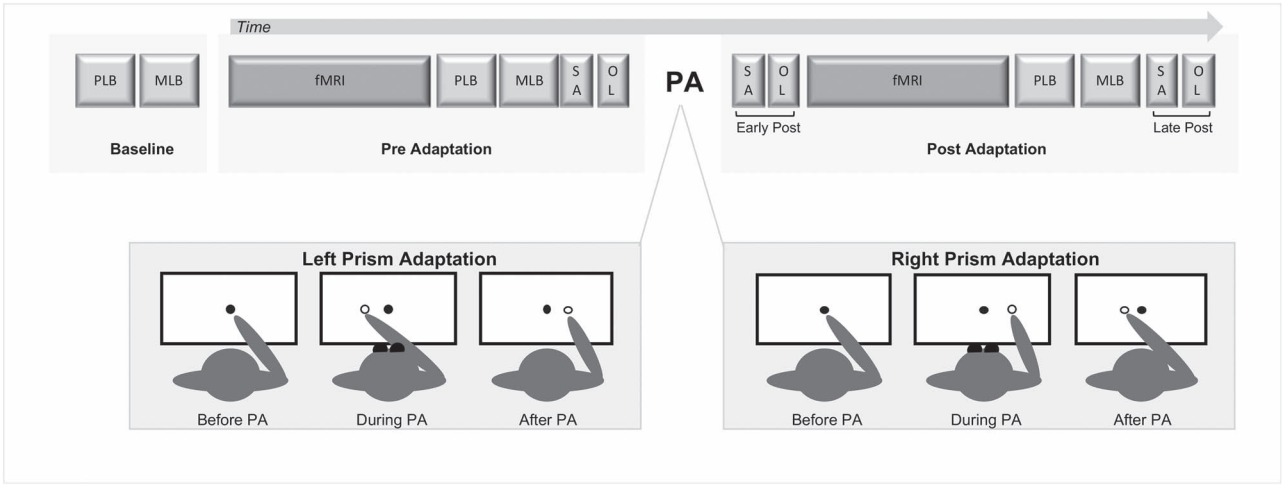

Figure 1. Experimental design. PLB = perceptual line bisection; MLB = manual line bisection; OL = open-loop pointing; SA = straight-ahead pointing; fMRI = functional magnetic resonance imaging; PA = prism adaptation.

movement. Participants were instructed to point with the index finger extended, in a single movement at a fast but comfortable speed, and to return the hand to the starting position.

Behavioral Assessment

Perceptual line bisection prioritizes the perceptual, and minimizes the motor component of the visuospatial bias by asking participants to judge a series or prebisected lines instead of actively bisecting them. We used a modified version of the Landmark task (Milner et al. 1992). The task consisted of 66 white, prebisected lines (350 × ~2 mm) displayed on a black screen positioned 35 cm from the eyes. Lines were transected at the true center and at 2, 4, 6, 8, and 10 mm to the left and right of the true center. Each of the 11 different prebisected lines was presented six times in a pseudorandom order, yielding a total of 66 trials, which took approximately 3 minutes to complete. Each line was displayed for a maximum of 5 seconds or until a response was made and was then replaced by a black-and-white, patterned mask, which stayed on the screen for 1 second before the next line was displayed. We used Presentation software (Neurobehavioral Systems, Inc.) to generate the stimuli, record responses, and control the task. Participants were instructed to inspect each line and judge whether the transecting mark was closer to the left or right end and to respond within 5 seconds by pressing pedals positioned under the left and right feet. We chose a pedal response to limit the use of the right hand, which was used for PA, since postadaptation feedback from that hand could contribute to de-adaptation. Subjects performed at least 10 practice trials before the baseline measurement. For each participant, we plotted the percentage of right-side responses as a function of the position of the transector (true center and 2, 4, 6, 8, and 10 mm to left and to the right of the true center). We then fit a sigmoid function to the data. The value on the x-axis corresponding to the point at which the participant responded with the right pedal 50% of the time was taken as the point of subjective equality (PSE).

Manual line bisection emphasizes the motor over the perceptual component of the visuospatial bias (Milner et al. 1992). We used this task to measure the visuospatial shift induced by PA (Schenkenberg et al. 1980). It consisted of a series of 10 black lines (identical in size to those used for the perceptual line bisection task) drawn on 297 × 420-mm sheets of paper, which were positioned over the same computer screen. Participants were instructed to inspect each line and, with a pen held in their right hand, draw a vertical mark at the perceived center of each line. No time limit was imposed and participants took on average of 1 second to place the mark on each line. We measured the distance between the mark placed by the participant and the true center of the line and took the average as the PSE, with marks to the right of center coded as positive.

Straight-ahead pointing was used to measure the proprioceptive shift induced by PA. Participants performed six pointing movements to the midline with the right index finger at a comfortable and uniform speed, while resting their left hands on their laps. Before each movement, participants were asked to close their eyes and imagine a line splitting their body in half and to project it onto the board in front of them. We then asked them to point to the line with their eyes closed and return to the starting position. To ensure that participants had no visual feedback, the arm and hand were occluded by a cardboard baffle before movement onset. The proprioceptive shift was measured as the average distance between the landing position and the true midline with precision of ± 0.5 cm.

Open-loop pointing was used to measure the sensorimotor shift induced by PA. Participants performed six pointing movements with the right index finger to the central (0°) target at a comfortable and uniform speed, while resting their left hands on their laps. The experimenter noted the landing position of the participant's finger with a precision of ± 0.5 cm. Before each movement, we instructed participants to look at the central target, close their eyes, point to the target while keeping their eyes closed, and then return the hand to the starting position. As in the straight-ahead task, vision of the arm and hand was occluded. We measured the sensorimotor shift as the average distance between the landing position and the central target.

fMRI

MRI Procedure

We acquired functional and structural MRI data with a 32-channel head coil on a research-dedicated 3-Tesla Siemens

MAGNETOM Prisma MR scanner. Head movement was minimized with padding. A whole-brain T1-weighted anatomical image (MPRAGE) was obtained for each participant (208 slices, voxel size 1.0 × 1.0 × 1.0 mm, repetition time (TR) = 2530 ms, echo time (TE) = 3.3 ms, TI = 1100 ms, field of view (FOV) = 256 × 256 × 208 mm, flip angle = 7°). T2* blood oxygen level-dependent (BOLD) resting state scans were acquired for all subjects (46 slices aligned to the AC-PC axis, voxel size 3.0 × 3.0 × 3.0 mm, TR = 2500 ms, TE = 30.0 ms, FOV = 192 × 138 × 192 mm, flip angle 70°, 64 × 46 × 64 acquisition matrix). During resting state scans, lighting was dimmed, and the subjects were instructed to lie still and look at a white central cross appearing on a black screen.

MRI Preprocessing

Functional and structural MRI data were preprocessed using the AFNI (version 18.2.15) software package (Cox 1996) and followed the general preprocessing approach of Wang et al. 2014. The anatomical scans were segmented into tissue compartments using Freesurfer. We removed the two initial volumes from each resting state scans to allow the magnetic field to stabilize. Volumes were then despiked (3dDespike), slice-time corrected to the first slice, coregistered to the anatomical scan and visually inspected for alignment accuracy, transformed to TT_N27 Template space (Talairach and Tournoux 1988), resampled to 2-mm isotropic voxels, smoothed with an isometric 4-mm full-width half-maximum Gaussian kernel, and scaled to percentage signal change (dividing each voxel's timeseries by its mean). TRs with head movement >0.3 mm were censored from the analysis, simultaneously with bandpass filtering (using 3dTproject) from 0.01 to 0.1 Hz. We regressed the six motion parameters and their derivatives, which were also filtered in the same manner (0.01–0.1 Hz) prior to performing the nuisance regression (Hallquist et al. 2013; Jo et al. 2013). Measures of mean frame-wise displacement (using the AFNI function @1dDiffMag) and average voxel-wise signal amplitude (standard deviation) were also calculated for use as nuisance covariates in group-level analyses in order to control for any residual global artifacts in the resting-state scans (Wang et al. 2014).

Functional Connectivity Analysis

To initiate the analysis, we created seed regions, within the posterior parietal cortex (PPC), composed of the right and left intraparietal sulcus (IPS) regions 1 and 2, where transcranial magnetic stimulation causes changes in visuospatial behavior when applied online (Szczepanski and Kastner 2013). We located these regions of interest using a probabilistic atlas of the visual areas (Wang et al. 2015). We created each seed by transforming the IPS 1 and 2 maps from the probabilistic atlas into TT_N27 template space and keeping voxels that had ≥30% probability of classification as being in IPS 1 or 2. We then combined the IPS 1 and 2 voxels to form a seed region (IPS 1–2; Fig. 3*a*). We created one seed in each hemisphere (left IPS 1–2 volume = 2984 mm^3, right IPS 1–2 volume = 2672 mm^3; Fig. 3*a*) and whole-brain time-series correlation maps from each seed. We used the Pearson correlation followed by Fisher's z-transform to improve normality. After functional MRI preprocessing, we created a brain mask for each participant, which included voxels with functional data present and excluded ventricles and white matter. We then created a group-level brain mask from these individual masks for use in group analyses, using voxels where at least 90% of participants had data.

Statistical Analysis

Statistical analyses were performed using SPSS (IBM, Version 24.0), R and Matlab (R2016a), and AFNI (3dLME command) with family-wise alpha set at 0.05. All data are presented as mean and the standard error (SEM). Effect sizes were computed as Cohen's *d*. When sphericity was violated, Greenhouse–Geisser-corrected values are reported. We used paired or independent *t*-tests for *post hoc* comparisons.

For each of the four behavioral measures, we performed a mixed analysis of variance (ANOVA) with time (pre, post or pre, early-post, late-post) as within-participant variables and group (left PA, right PA) as between participant variables. To assess the changes in RSFC, data were submitted to a linear mixed effects regression model (LMER) with seed-based functional connectivity (correlation maps) as the dependent variable, and group (left PA, right PA), time (pre, post), and hemisphere (left, right) as fixed effects, subject as a random effect, and motion (@1dDiffMag) and average voxel-wise standard deviation as nuisance covariates.

Results

Behavior

Independent paired *t*-tests comparing performance at baseline between the left and right PA groups for each of the four behavioral tasks revealed a significant difference only for the open-loop pointing task ($t(36) = -2.199$, $P = 0.034$, Cohen's $d = 0.70$; all other $t(36) \leq 1.585$ $P \leq 0.122$).

Open-Loop Pointing

We measured sensorimotor performance by quantifying the deviation in pointing from the landing position and the true center, before (pre) immediately after postadaptation (early-post), and at the end of the experiment (late-post). The mixed time × group ANOVA revealed a significant main effect of group ($F(1, 36) = 78.363$, $P = 0.002$, $\eta^2_p = 0.68$), such that the pointing error was right of the center (mean = 2.164 cm) for the left PA group and left of the center (−1.795 cm) for the right PA group (Fig. 2*a*). There was a significant time × group interaction ($F(2, 36) = 284.031$, $P < 0.001$, $\eta^2_p = 0.89$) and a nonsignificant main effect of time ($F(2, 36) = 1.169$, $P = 0.317$). To further analyze the significant time × group interaction, we performed a follow-up repeated-measures ANOVA for time for each group, which revealed main effects of time for both the left ($F(2, 19)$ 193.373 $P < 0.001$, $\eta^2_p = 0.91$) and right PA ($F(2, 17) = 106.951$, $P < 0.001$, $\eta^2_p = 0.86$) groups. The left PA group showed a rightward shift in pointing at both the early (4.86 cm) ($t(19) = -17.228$, $P < 0.001$, Cohen's $d = -3.85$) and late (1.92 cm) ($t(19) = -9.703$, $P < 0.001$, Cohen's $d = -2.17$) post measurements. The right PA group exhibited a leftward shift at the early-post (−4.22 cm) ($t(17) = -12.196$, $P < 0.001$, Cohen's $d = 2.73$) and late-post (−1.93 cm) ($t(17) = 9.694$, $P < 0.001$, Cohen's $d = 2.17$) measurements. Independent *t*-tests on the absolute values of change found no significant difference between the groups in the size of the shift at either the early ($t(36) = 0.470$, $P = 0.641$) or late ($t(36) = -1.137$, $P = 0.263$) post measurements. Since there was a difference in performance between the two groups at baseline, we ran a mixed time × group ANOVA with the change in pointing as the dependent measure and baseline pointing as a covariate. This revealed a significant time × group interaction ($F(1, 35) = 4.297$, $P = 0.046$, $\eta^2_p = 0.11$) and a nonsignificant time × baseline interaction ($F(1, 35) = 2.610$, $P = 0.115$, $\eta^2_p = 0.06$),

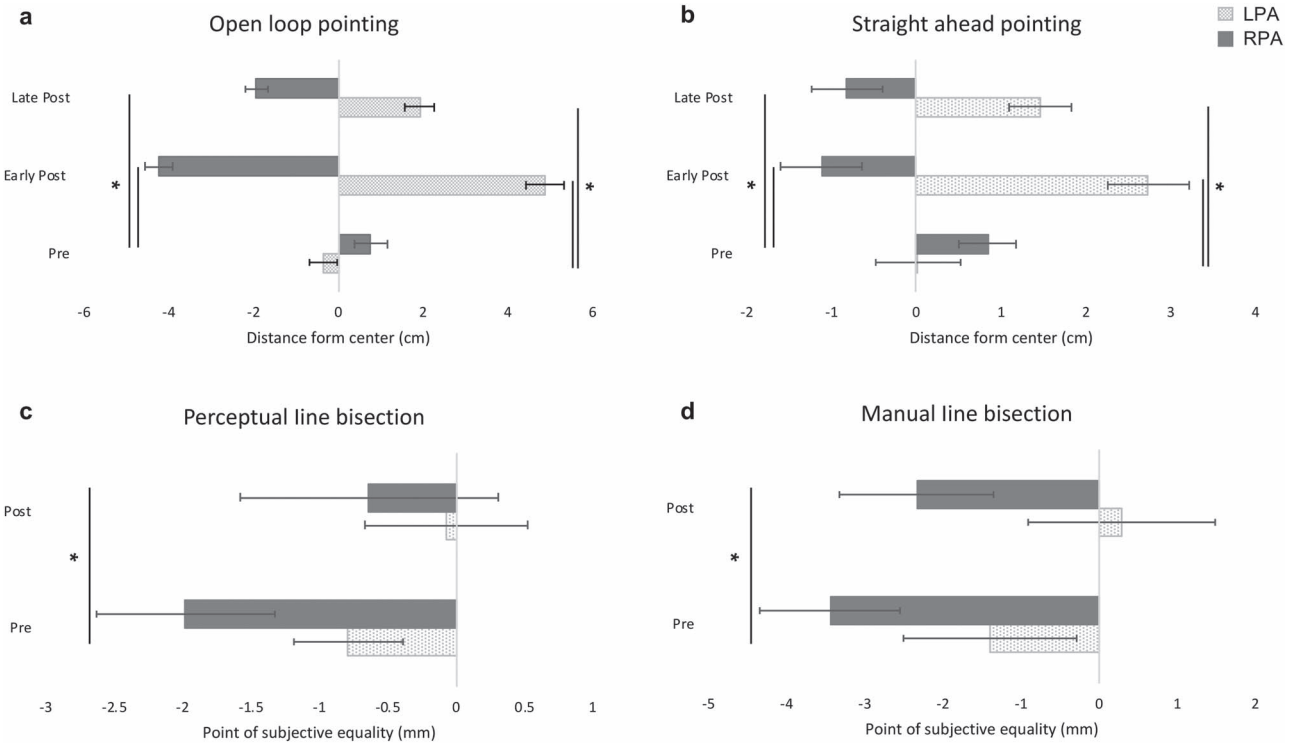

Figure 2. Behavioral effects of prism adaptation. Negative and positive values represent left and right of center, respectively. Error bars represent 1 SEM. *$P < 0.05$.

showing that the baseline difference between the groups was unlikely to be the source of the time × group interaction.

Straight-Ahead Pointing

We measured proprioceptive performance by quantifying the deviation in the pointing between the perceived and true midline. The mixed effects time × group ANOVA revealed a significant main effect of group ($F(1, 36) = 11.661$, $P = 0.002$, $\eta^2_p = 0.24$; Fig. 2*b*). Again, the pointing error was rightward for the left PA group (1.404 cm) and leftward for the right PA group (−0.363 cm). There was a significant time × group interaction ($F(2, 36) = 33.754$, $P < 0.001$ $\eta^2_p = 0.48$) and a nonsignificant main effect of time ($F(2, 36) = 1.534$, $P = 0.223$). Follow-up repeated measures ANOVAs, performed individually for each group, found a significant main effect of time for both left PA ($F(2, 19) = 27.669$, $P < 0.001$, $\eta^2_p = 0.59$) and right PA ($F(2, 17) = 10.729$, $P < 0.001$, $\eta^2_p = 0.39$). The left PA group had a rightward shift in pointing at both the early (2.733 cm) ($t(19) = -6.176$, $P < 0.001$, Cohen's $d = -1.38$) and late (−1.458) ($t(19) = -4.604$, $P < 0.001$, Cohen's $d = -1.03$) post measurements and right PA group pointing shifted leftward at the early (−1.120 cm) ($t(17) = 4.182$, $P = 0.001$, Cohen's $d = 0.93$) and late (−0.815 cm) ($t(1, 17) = 4.880$, $P < 0.001$, Cohen's $d = 1.09$) time points. Independent *t*-tests comparing the absolute value of change revealed no significant difference in the aftereffect between the two groups at the early ($t(36) = 0.676$, $P = 0.503$) and late ($t(36) = -0.510$, $P = 0.613$) post measurements.

Perceptual Line Bisection

We averaged the two preadaptation scores since they did not differ ($t(36) = 1.585$, $P = 0.122$). The mixed time × group ANOVA found a significant main effect of time ($F(1, 36) = 5.363$, $P = 0.026$, $\eta^2_p = 0.13$; Fig. 2*c*). The two groups combined shifted their midline judgment rightward (from −1.317 mm to—0.338 mm) after PA. The time × group interaction was not significant ($F(1, 36) = 0.491$, $P = 0.488$).

Manual Line Bisection

For the perceptual line bisection task, we averaged the two preadaptation scores since they did not differ ($t(36) = 1.418$ $P = 0.165$). The mixed time × group ANOVA showed a main effect of time ($F(1, 36) = 9.101$, $P = 0.005$, $\eta^2_p = 0.202$). PA produced a rightward bias in midline judgment independent of PA direction (from −2.365 mm to −0.958 mm). The time × group interaction was not significant ($F(1, 36) = 0.378$, $P = 0.543$).

Resting State Functional Connectivity

Before covarying head motion and the average standard deviation nuisance measures in the LMER, we ascertained that those variables did not differ between the RPA and LPA groups at baseline (motion $t(36) = -0.119$, $P = 0.906$; standard deviation $t(36) = 1.004$, $P = 0.322$; RPA: motion mean = 0.062 (SEM = 0.008), standard deviation = 0.826 (0.110); LPA: motion = 0.064 (0.007), standard deviation = 0.785 (0.141)) or at post (motion $t(36) = 0.129$, $P = 0.898$; standard deviation $t(36) = -0.434$, $P = 0.667$; RPA: motion = 0.060 (0.008), standard deviation = 0.790 (0.021); LPA: motion 0.059 (0.005), standard deviation = 0.806 (0.028)). Similarly, the within comparison did not reveal any difference between pre- and post-PA phases for both the RPA (motion $t(17) = -0.276$, $P = 0.786$; standard deviation $t(17) = -1.503$, $P = 0.151$) and LPA groups (motion $t(19) = -1.041$, $P = 0.311$; standard deviation $t(19) = 0.962$, $P = 0.348$).

Table 1 Clusters surviving the group × time interaction (FDR corrected $q < 0.05$; $P < 0.05$)

	Volume (mm^3)	Peak (X)	Peak (y)	Peak (z)	Brain region
1	520	21	–43	0	Right parahippocampal gyrus
2	288	–17	–55	–14	Left declive
3	264	53	–3	14	Right precentral gyrus
4	200	53	3	28	Right precentral gyrus/inferior frontal gyrus
5	192	–55	–43	6	Left superior temporal gyrus
6	184	17	–63	–12	Right declive
7	176	–3	–29	–8	(Within 6 mm) left red nucleus
8	168	–37	–23	–14	Left parahippocampal gyrus

Coordinates are in Talairach–Tournoux space.

Right versus Left PA Contrast

The LMER analysis revealed a significant group × time interaction (false discovery rate (FDR) corrected to $P < 0.05$; $q < 0.05$), such that RSFC was differentially affected according to PA direction. The analysis detected 8 significant clusters relative to the IPS seeds (Table 1 and Fig. 3*b*). We included any clusters with 20 or more voxels in subsequent analyses in order to avoid post hoc testing in small, noisy clusters.

To follow up the group × time interaction, we extracted the time series of each cluster that survived the LMER for each group separately. We computed correlations between each cluster time series and the averaged time series of the IPS 1–2 seeds. We then compared the Fisher *z*-transformed correlation coefficient before and after PA. Post hoc testing (paired *t*-tests) of the correlation coefficients revealed that the time × group interaction was characterized mainly by a decrease in RSFC between the IPS seeds and other brain regions, and that the changes were specific to the PA direction, as shown in Fig. 3*c*. Right and left PA had differential effects on RSFC between the IPS seeds and the parahippocampal gyri. Right PA caused a decrease in RSFC between the seeds and a cluster including the posterior portion of the right parahippocampal gyrus, the fusiform and lingual gyri, and extending to the thalamus ($t(17) = 4.367$, $P < 0.001$, Cohen's $d = 1.03$). The left PA group showed a decrease in connectivity between the IPS seeds and a cluster including the anterior portion of the left parahippocampal gyrus and extending to the hippocampus ($t(19) = 2.531$, $P = 0.02$, Cohen's $d = 0.57$). The right PA group also showed changes in RSFC between the IPS seeds and the superior temporal gyrus ($t(17) = 2.617$, $P = 0.018$, Cohen's $d = 0.62$), red nucleus ($t(17) = 2.939$, $P = 0.009$, Cohen's $d = 0.569$), the left ($t(17) = 4.176$, $P = 0.001$, Cohen's $d = 0.98$) and right ($t(17) = 4.646$, $P < 0.001$, Cohen's $d = 1.09$) cerebellum. By contrast, the left PA group showed a decrease in RSFC between the seeds and the right precentral ($t(19) = 2.252$, $P = 0.036$, Cohen's $d = 0.50$) and inferior frontal gyri ($t(19) = 2.360$, $P = 0.029$, Cohen's $d = 0.53$). Following FDR correction ($q < 0.05$, *P*-value threshold = 0.009), only the following clusters survived and only in the right PA group: fusiform and lingual gyri and extending to the thalamus ($t(17) = 4.367$, $P < 0.001$, Cohen's $d = 1.03$), and the left ($t(17) = 4.176$, $P = 0.001$, Cohen's $d = 0.98$) and right ($t(17) = 4.646$, $P < 0.001$, Cohen's $d = 1.09$) cerebellum.

Single-Group Contrasts

There were differential changes in RSFC between the IPS seeds and other brain structures, which did not survive the whole brain analysis but did survive the single-group contrasts, corrected for whole-brain contrasts (FDR corrected $q < 0.05$; voxelwise threshold $P = 0.0051$). As reported in Table 2, the separate contrasts (post vs. pre) for each group revealed that both left and right PA decreased RSFC between IPS seeds and the superior temporal gyrus (STG) bilaterally (Fig. 4*a*1, *a*2, *b*1 and *b*2). Right PA increased RSFC between the IPS seeds and the right middle frontal gyrus (MFG; Fig. 4*a*3), and left PA decreased it (Fig. 4*b*3). Right PA increased RSFC between the IPS seeds and inferior parietal lobule bilaterally (IPL; Fig. 4*a*4 and *a*5), and left PA decreased RSFC between the IPS seeds and the left IPL (Fig. 4*b*4), and between the IPS seeds and the right superior parietal lobule (SPL; Fig. 4*b*5). See Supplementary Tables S1 (right PA) and S2 (left PA) for a full list of significant clusters. For further analysis, see Supplementary Table S3.

Discussion

We investigated the effect of PA on RSFC at the whole brain level by contrasting left and right PA in two groups of healthy participants and found differential changes in a cerebellar-parieto-parahippocampal network in the right hemisphere, depending on the direction of adaptation (Fig. 3 and Table 1). The single-group contrast revealed that while left and right PA elicited opposite changes in RSFC between regions within both PPCs and between the frontal and parietal areas involved in visuospatial function, the direction of change was the same between the seed and temporal areas (Fig. 4 and Table 2, Supplementary Tables S1 and S2).

Behavioral Results

As expected, left PA produced a rightward shift, and right PA produced a leftward shift, in sensorimotor and proprioceptive pointing performance. These aftereffects were of similar magnitude so any differences in the imaging results cannot be attributed to a difference in the degree of adaptation. The aftereffects were still present at the end of the experiment, meaning that adaptation lasted throughout the fMRI data acquisition and visuospatial behavioral assessment.

While we expected a rightward bias (neglect-like behavior) on the perceptual line bisection task after left, but not right, PA (Colent et al. 2000; McIntosh et al. 2019), there was a significant rightward shift in midline judgment, independent of PA direction, on both the perceptual and manual line bisection tasks. Since the absence of a time × group interaction made *post hoc* comparison inappropriate, we do not know whether these shifts were individually significant. The lack of a significant rightward shift after left PA could be due to fluctuations in the

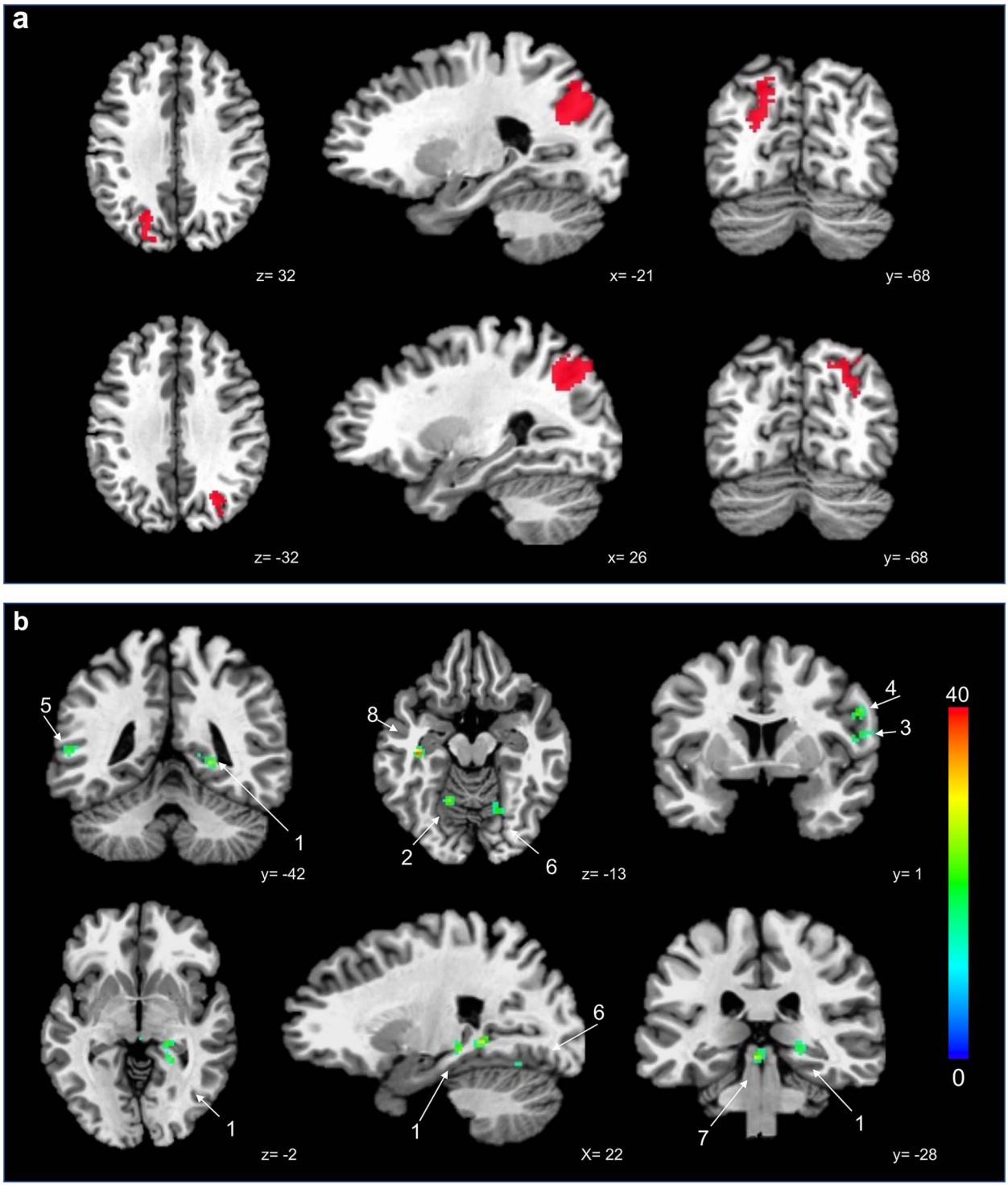

Figure 3. *a*: Locations of left and right IPS 1–2 seeds *b*: Brain regions with significant clusters of RSFC change resulting from the group × time interaction (FDR corrected, $P < 0.05$). Color scale indicates *F*-value. Numbers refer to clusters in Table 1. *c*: Amount of change (post-pre) in RSFC between each cluster in A and the IPS 1–2 seeds. Error bars = 1 SEM. $^{*}P < 0.001$ and surviving FDR correction. Cluster threshold = 20 voxels. $^{*}P < 0.05$.

cognitive aftereffect (Schintu et al. 2014). In any case, the absence of a significant effect on line bisection would not invalidate the effects on RSFC, since others, such as Crottaz-Herbette et al. (2014) have reported significant effects of PA on brain activity without significant behavioral changes.

Neuroimaging Results

Right versus Left PA Contrast

Compared with left PA, right PA decreased RSFC between a portion of the PPC (the IPS 1–2 seeds) and the parahippocampal gyrus, and between the seed and the cerebellum (Fig. 3

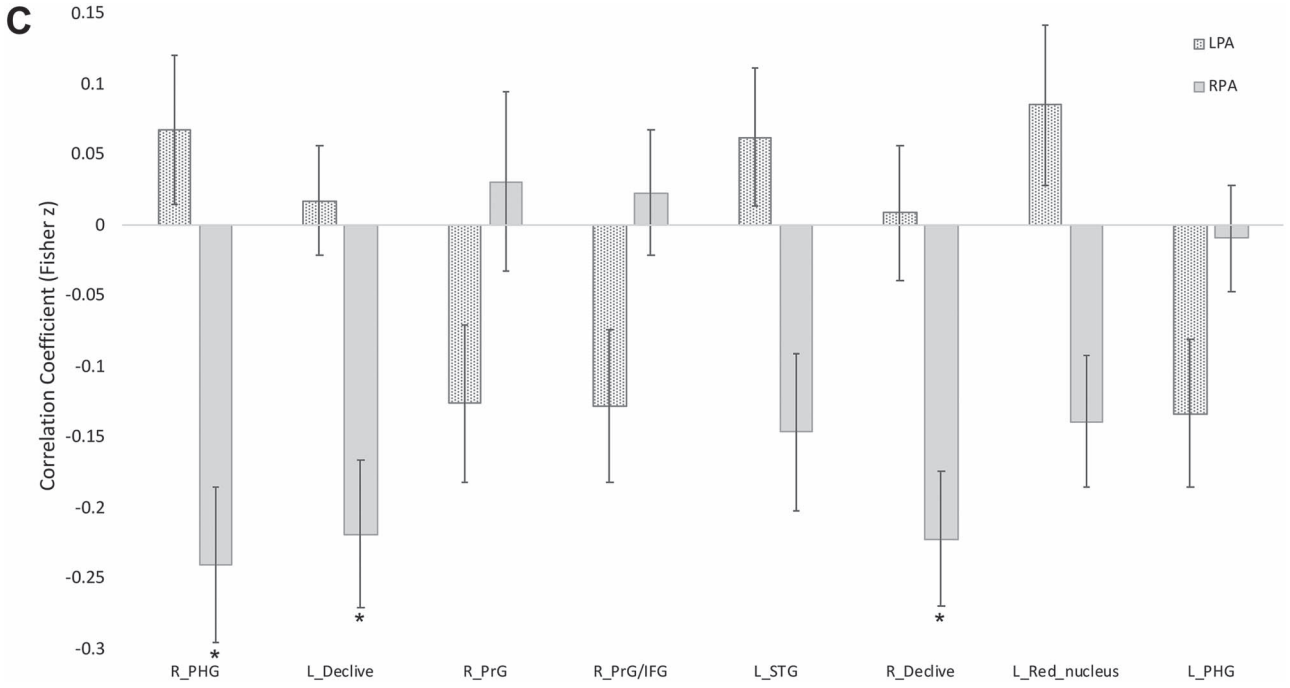

Figure 3. Continued.

Table 2 Contrast (post–pre) for right and left PA

Volume (mm^3)	Peak (X)	Peak (y)	Peak (z)	Brain region	Direction of change
				Right prism adaptation	
1064	47	5	-22	Right superior temporal gyrus	Down
864	35	43	22	Right middle frontal gyrus	Up
864	–45	–3	–10	Left superior temporal gyrus	Down
480	49	–47	46	Right inferior parietal lobule	Up
432	–45	–63	44	Left inferior parietal lobule	Up
				Left prism adaptation	
3968	53	1	40	Right middle frontal gyrus	Down
2688	–45	–33	26	Left inferior parietal lobule	Down
1632	29	–59	46	Right superior parietal lobule	Down
408	45	–5	–8	Right superior temporal gyrus	Down
256	–45	–29	2	Left superior temporal gyrus	Down

Coordinates are in Talairach–Tournoux space. BA = Brodmann area.

and Table 1), all of which are involved in spatial navigation (Aguirre et al. 1996; Aguirre and D'Esposito 1997; Maguire et al. 1998; Grön et al. 2000; Rondi-Reig and Burguière 2005). The PPC, which contains egocentric (body-referenced) representations (Silver and Kastner 2009), may feed spatial information to the parahippocampal cortex, which is important for allocentric (world-referenced) representation (Aguirre and D'Esposito 1999). The PPC appears to transform the allocentric output of the hippocampus and other medial temporal lobe structures into egocentric coordinates to support movement through the environment (Whitlock et al. 2008; Kravitz et al. 2011).

RSFC between a portion of the PPC and parahippocampal gyrus decreased following right PA, suggesting that reduced communication between these areas reflects modulation of the egocentric reference frame in the navigation network. The cerebellum is not only involved in spatial navigation (Malm et al. 1998; Schmahmann and Sherman 1998; Molinari et al. 2004), but linked with brainstem and thalamic structures concerned with oculomotor control and the vestibular system (Schmahmann 2010), which encodes self-orientation with respect to gravity. Further support for the involvement of the cerebellum in the egocentric spatial reference frame comes from the finding that the hippocampus and cerebellum interacted only during a navigation task based on an egocentric representation and not when the reference was allocentric (Iglói et al. 2015). Vestibular information is fed from the cerebellum into the navigation network through the hippocampus (Rochefort et al. 2013), perhaps via a multisynaptic pathway involving the PPC (Rochefort et al. 2013)

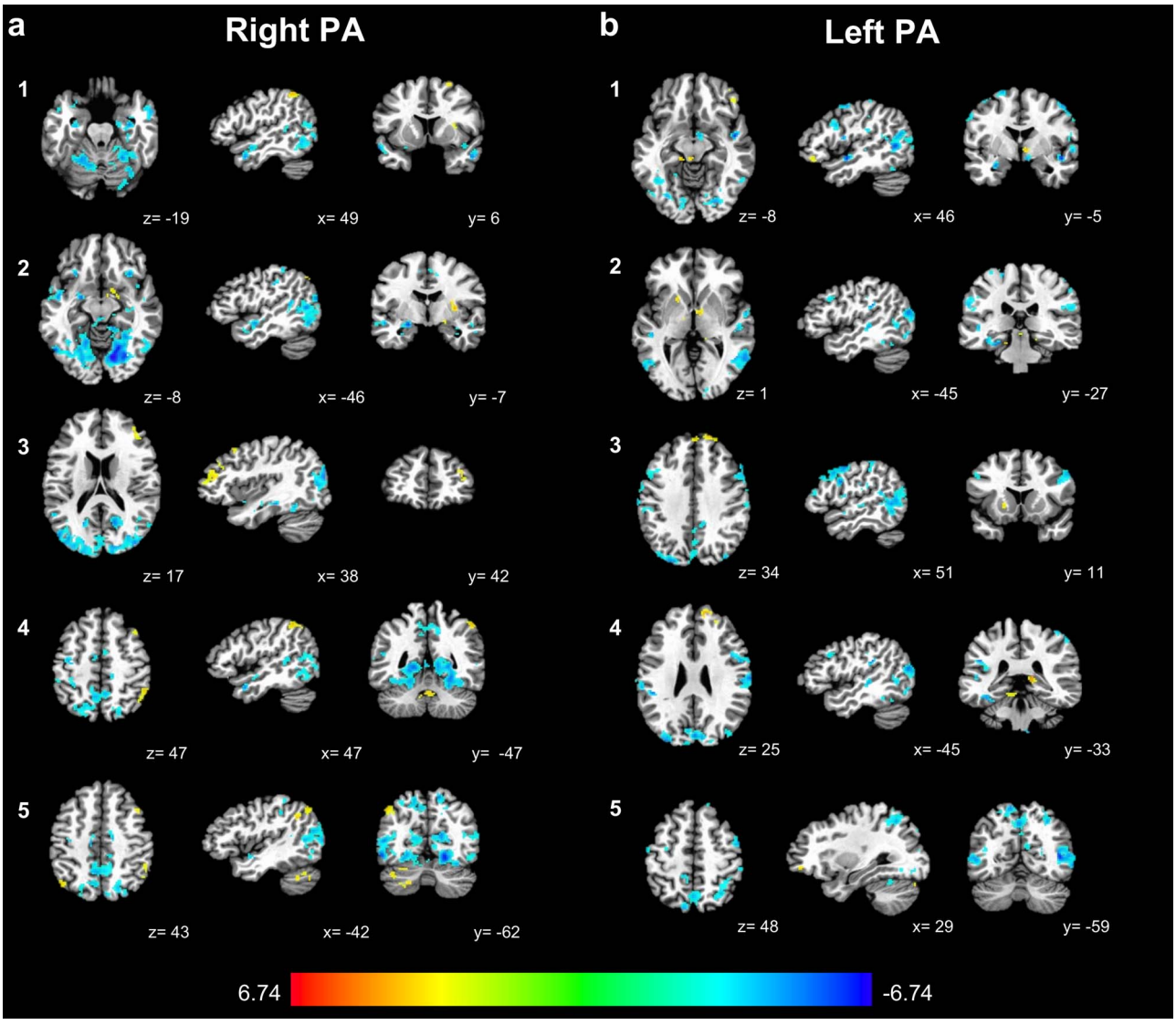

Figure 4. Contrast (post vs. pre) z-score for the right (*a*) and left (*b*) PA groups (FDR $q < 0.05$, $P < 0.0052$). Color scale indicates z-value; warm colors: RSFC increases with IPS 1–2; cool colors: decreases.

or directly from Lobule VI (Watson et al. 2019). According to the conventional model of PA (Pisella et al. 2006), and given its connection with the PPC (Casula et al. 2016), it is possible that the cerebellum supplies egocentric spatial data to the PPC in a bottom-up process. The cerebellum is known to be involved in visuo-motor transformation learning (Graydon et al. 2005), which is required for the PA adaptation phase. However, we found that the changes in RSFC between cerebellum and PPC outlasted adaptation and persisted in the aftereffect phase. This novel result fits with clinical data on spatial processing deficits after cerebellar damage and the emerging concept of cerebellar involvement in cognition (Rondi-Reig and Burguière 2005).

The first level of analysis, contrasting right and left PA, revealed different effects on RSFC between the PPC and parahippocampal cortex and between the PPC and cerebellum, structures that, along with the hippocampus, comprise the navigation network. Based on this result, we suggest that right PA, by downregulating connectivity between the PPC and the cerebellum, may alter vestibular input, and, by decreasing those inputs between the PPC and right parahippocampal gyrus, further change the influence of egocentric spatial information. This effect on the spatial reference frame may explain how right PA improves the complex of symptoms in neglect. Vestibular input is important for maintaining spatial orientation (Ventre-Dominey et al. 1999; Doricchi et al. 2002) and plays a role in neglect (Cappa et al. 1987; Vallar et al. 1993). For example, irrigation of the right ear with cold water, to cause convection in the endolymph of the vestibular apparatus and stimulate vestibular signaling, improves spatial functioning in neglect patients. Vestibular stimulation, especially when combined with activation of neck muscle stretch receptors, another source of positional information, by vibration, provides the sensory signals needed to create a spatial frame of reference based on eye and head position in space (Karnath 1994). Eye and head position perception is compromised in neglect. Since neglect patients have impaired vestibular signaling to the

IPS, egocentric spatial information relayed to the PPC may be inaccurate. Right PA could act upon those erroneous inputs and partially restore spatial perception. However, the nature of the RPA-induced egocentric reference frame modulation and its effect on behavior remain to be further clarified.

Single-Group Contrast

The contrast between the effects of left and right PA revealed those brain regions whose RSFC changes differed between the two PA directions and survived whole brain correction. However, *post hoc* analysis allowed us to look at changes in RSFC before and after PA within each group separately. There were widespread changes in RSFC for both PA groups (Supplementary Tables S1 and S2), but here we limit discussion to those brain structures whose involvement in PA has been previously reported in the literature (parietal, frontal and temporal regions). At the single-group level, right PA increased RSFC between areas within the PPCs, and left PA decreased it (Fig. 4 and Table 2). That is, PA had a bilateral effect on local connectivity within the PPC, consistent with previous findings (Saj et al. 2013) showing a bilateral increase of task-related activation in parietal areas and the direction of the change depended on the direction of the visual displacement in agreement with the current model of neglect (Pisella et al. 2006; Striemer and Danckert 2010). Right PA increased, and left PA decreased, RSFC between the seeded portion of the PPC and the MFG. The posterior IPS is the node of the dorsal attentional network receiving the most input from the ventral attentional network, possibly via the right MFG, which is thought to be the link between the two networks (Corbetta et al. 2008). Activity in the right MFG correlates with activity of both attention networks (Fox et al. 2006), and disconnection in the right ventral attention network is strongly related to the severity of neglect (He et al. 2007). This is consistent with the effect of PA on frontoparietal RSFC in our data. Finally, both left and right PA decreased RSFC between the seed in the PPC and the STG bilaterally. The STG, where damage causes neglect (Karnath et al. 2001, 2004), is involved in visual attention, and has been affected by PA in previous studies (Luaute et al. 2006; Crottaz-Herbette et al. 2017) and our result supports its involvement in PA aftereffect.

In conclusion, we propose that the decrease in RSFC in the right parieto-cerebellar-parahippocampal navigation network caused by right PA reflects modulation of egocentrically referenced input to the navigation network. The results of the single contrast analysis provide evidence for the action of PA on the frontoparietal network and within the PPCs and also refine the existing model (Pisella et al. 2006; Striemer and Danckert 2010). In agreement with the model, we found that right and left PA cause opposite changes in RSFC, i.e., right PA increases it and left PA decreases it. However, the directions of those changes are the same across hemispheres. Consistent with previous studies, we propose that right PA may reduce visuospatial neglect by increasing connectivity between the IPS and frontoparietal cortex in the lesioned right hemisphere, and left PA may induce neglect-like behavior in healthy individuals by decreasing frontoparietal connectivity on the right. In both cases, PA reduces the influence of temporal over posterior parietal regions. These results not only help resolve contradictions in the literature concerning the neural changes caused by right and left PA, but also expand the effect of PA on the spatial navigation network and extend the role of the cerebellum from the adaptation phase to the aftereffect phase.

Supplementary Material

Supplementary material can be found at *Cerebral Cortex* online.

Funding

National Institutes of Health Ruth L. Kirschstein National Research Service to S.S., the National Science Foundation (grants BCS-1534823 and BCS-1921415 to S.S.); Center for Neuroscience and Regenerative Medicine (CNRM-70-3904 to M.F.); Intramural Research Programs of the National Institute of Mental Health to S.J.G. and the National Institute of Neurological Disorders and Stroke (1ZIANS002977–20 to E.M.W.).

Notes

Conflict of Interest: The authors declare no conflict of interest.

References

Aguirre GK, D'Esposito M. 1997. Environmental knowledge is subserved by separable dorsal/ventral neural areas. *J Neurosci*. 17:2512–2518.

Aguirre GK, D'Esposito M. 1999. Topographical disorientation: a synthesis and taxonomy. *Brain*. 122:1613–1628.

Aguirre GK, Detre JA, Alsop DC, D'Esposito M. 1996. The parahippocampus subserves topographical learning in man. *Cereb Cortex*. 6:823–829.

Anelli F, Frassinetti F. 2019. Prisms for timing better: a review on application of prism adaptation on temporal domain. *Cortex*. 119:583–593.

Azouvi P, Jacquin-Courtois S, Luauté J. 2017. Rehabilitation of unilateral neglect: evidence-based medicine. *Ann Phys Rehabil Med*. 60:191–197.

Bowers D, Heilman KM. 1980. Pseudoneglect: effects of hemispace on a tactile line bisection task. *Neuropsychologia*. 18:491–498.

Cappa S, Sterzi R, Vallar G, Bisiach E. 1987. Remission of hemineglect and anosognosia during vestibular stimulation. *Neuropsychologia*. 25:775–782.

Casula EP, Pellicciari MC, Ponzo V, Stampanoni Bassi M, Veniero D, Caltagirone C, Koch G. 2016. Cerebellar theta burst stimulation modulates the neural activity of interconnected parietal and motor areas. *Sci Rep*. 6:36191.

Chapman HL, Eramudugolla R, Gavrilescu M, Strudwick MW, Loftus A, Cunnington R, Mattingley JB. 2010. Neural mechanisms underlying spatial realignment during adaptation to optical wedge prisms. *Neuropsychologia*. 48:2595–2601.

Clarke S, Crottaz-Herbette S. 2016. Modulation of visual attention by prismatic adaptation. *Neuropsychologia*. 92:31–41.

Clower DM, Hoffman JM, Votaw JR, Faber TL, Woods RP, Alexander GE. 1996. Role of posterior parietal cortex in the recalibration of visually guided reaching. *Nature*. 383:618–621.

Colent C, Pisella L, Bernieri C, Rode G, Rossetti Y. 2000. Cognitive bias induced by visuo-motor adaptation to prisms: a simulation of unilateral neglect in normal individuals? *Neuroreport*. 11.

Corbetta M, Patel G, Shulman GL. 2008. The reorienting system of the human brain: from environment to theory of mind. *Neuron*. 58:306–324.

Corbetta M, Shulman GL. 2002. Control of goal-directed and stimulus-driven attention in the brain. *Nat Rev Neurosci*. 3:201–215.

Cox RW. 1996. AFNI: software for analysis and visualization of functional magnetic resonance neuroimages. *Computers and Biomedical Research*. 29:162–173.

Crottaz-Herbette S, Fornari E, Clarke S. 2014. Prismatic adaptation changes visuospatial representation in the inferior parietal lobule. *J Neurosci*. 34:11803–11811.

Crottaz-Herbette S, Fornari E, Notter MP, Bindschaedler C, Manzoni L, Clarke S. 2017. Reshaping the brain after stroke: the effect of prismatic adaptation in patients with right brain damage. *Neuropsychologia*. 104:54–63.

Doricchi F, Siegler I, Iaria G, Berthoz A. 2002. Vestibulo-ocular and optokinetic impairments in left unilateral neglect. *Neuropsychologia*. 40:2084–2099.

Fox MD, Corbetta M, Snyder AZ, Vincent JL, Raichle ME. 2006. Spontaneous neuronal activity distinguishes human dorsal and ventral attention systems. *Proc Natl Acad Sci*. 103:10046–10051.

Graydon FX, Friston KJ, Thomas CG, Brooks VB, Menon RS. 2005. Learning-related fMRI activation associated with a rotational visuo-motor transformation. *Cogn Brain Res*. 22: 373–383.

Grön G, Wunderlich AP, Spitzer M, Tomczak R, Riepe MW. 2000. Brain activation during human navigation: gender-different neural networks as substrate of performance. *Nat Neurosci*. 3:404.

Hallquist MN, Hwang K, Luna B. 2013. The nuisance of nuisance regression: spectral misspecification in a common approach to resting-state fMRI preprocessing reintroduces noise and obscures functional connectivity. *NeuroImage*. 82:208–225.

He BJ, Snyder AZ, Vincent JL, Epstein A, Shulman GL, Corbetta M. 2007. Breakdown of functional connectivity in frontoparietal networks underlies behavioral deficits in spatial neglect. *Neuron*. 53:905–918.

Helmholtz H. 1867. Handbuch der physiologischen optik. In: Voss L, editor. *Published in English as Treatise on Physiological Optics, vol. 3, trans*. Leipzig: J Southal Opt Soc Am.

Iglói K, Doeller CF, Paradis A-L, Benchenane K, Berthoz A, Burgess N, Rondi-Reig L. 2015. Interaction between hippocampus and cerebellum crus I in sequence-based but not place-based navigation. *Cereb Cortex*. 25:4146–4154.

Jo HJ, Gotts SJ, Reynolds RC, Bandettini PA, Martin A, Cox RW, Saad ZS. 2013. Effective preprocessing procedures virtually eliminate distance-dependent motion artifacts in resting state FMRI. *J Appl Math*. doi: 10.1155/2013/935154.

Karnath HO. 1994. Subjective body orientation in neglect and the interactive contribution of neck muscle proprioception and vestibular stimulation. *Brain J Neurol*. 117(Pt 5): 1001–1012.

Karnath H-O, Ferber S, Himmelbach M. 2001. Spatial awareness is a function of the temporal not the posterior parietal lobe. *Nature*. 411:950–953.

Karnath H-O, Fruhmann Berger M, Küker W, Rorden C. 2004. The anatomy of spatial neglect based on voxelwise statistical analysis: a study of 140 patients. *Cereb Cortex*. 14:1164–1172.

Kravitz DJ, Saleem KS, Baker CI, Mishkin M. 2011. A new neural framework for visuospatial processing. *Nat Rev Neurosci*. 12:217–230.

Küper M, Wünnemann MJS, Thürling M, Stefanescu RM, Maderwald S, Elles HG, Göricke S, Ladd ME, Timmann D. 2014. Activation of the cerebellar cortex and the dentate nucleus in a prism adaptation fMRI study. *Hum Brain Mapp*. 35: 1574–1586.

Luaute J, Michel C, Rode G, Pisella L, Jacquin-Courtois S, Costes N, Cotton F, le Bars D, Boisson D, Halligan P *et al*. 2006. Functional anatomy of the therapeutic effects of prism adaptation on left neglect. *Neurology*. 66:1859–1867.

Luauté J, Schwartz S, Rossetti Y, Spiridon M, Rode G, Boisson D, Vuilleumier P. 2009. Dynamic changes in brain activity during prism adaptation. *J Neurosci*. 29:169–178.

Magnani B, Caltagirone C, Oliveri M. 2014. Prismatic adaptation as a novel tool to directionally modulate motor cortex excitability: evidence from paired-pulse TMS. *Brain Stimul*. 7:573–579.

Maguire EA, Burgess N, Donnett JG, Frackowiak RSJ, Frith CD, O'Keefe J. 1998. Knowing where and getting there: a human navigation network. *Science*. 280:921–924.

Malm J, Kristensen B, Karlsson T, Carlberg B, Fagerlund M, Olsson T. 1998. Cognitive impairment in young adults with infratentorial infarcts. *Neurology*. 51:433.

McIntosh RD, Brown BMA, Young L. 2019. Meta-analysis of the visuospatial aftereffects of prism adaptation, with two novel experiments. *Cortex*. 111:256–273.

Michel C. 2016. Beyond the sensorimotor plasticity: cognitive expansion of prism adaptation in healthy individuals. *Front Psychol*. 6:1979. doi: 10.3389/fpsyg.2015.01979.

Miles WR. 1930. Ocular dominance in human adults. *J Gen Psychol*. 3:412–430.

Milner AD, Brechmann M, Pagliarini L. 1992. To halve and to halve not: an analysis of line bisection judgements in normal subjects. *Neuropsychologia*. 30:515–526.

Milner AD, Goodale MA. 2006. *The Visual Brain in Action*. Oxford; New York: Oxford University Press.

Molinari M, Petrosini L, Misciagna S, Leggio MG. 2004. Visuospatial abilities in cerebellar disorders. *J Neurol Neurosurg Psychiatry*. 75:235–240.

Oldfield RC. 1971. The assessment and analysis of handedness: the Edinburgh inventory. *Neuropsychologia*. 9:97–113.

Pisella L, Rode G, Farnè A, Tilikete C, Rossetti Y. 2006. Prism adaptation in the rehabilitation of patients with visuo-spatial cognitive disorders. *Curr Opin Neurol*. 19:534–542.

Rochefort C, Lefort JM, Rondi-Reig L. 2013. The cerebellum: a new key structure in the navigation system. *Front Neural Circuits*. 7:35. https://www.frontiersin.org/articles/10.3389/fncir.2013.00035/full (last accessed 14 April 2019).

Rondi-Reig L, Burguière E. 2005. Is the cerebellum ready for navigation? In: *Progress in Brain Research*. Creating Coordination in the Cerebellum: Elsevier, pp. 199–212 http://www.sciencedirect.com/science/article/pii/S0079612304480170 (last accessed 30 October 2019).

Rossetti Y, Rode G, Pisella L, Farné A, Li L, Boisson D, Perenin MT. 1998. Prism adaptation to a rightward optical deviation rehabilitates left hemispatial neglect. *Nature*. 395:166–169.

Saj A, Cojan Y, Vocat R, Luauté J, Vuilleumier P. 2013. Prism adaptation enhances activity of intact fronto-parietal areas in both hemispheres in neglect patients. *Cortex*. 49:107–119.

Schenkenberg T, Bradford DC, Ajax ET. 1980. Line bisection and unilateral visual neglect in patients with neurologic impairment. *Neurology*. 30:509–517.

Schintu S, Freedberg M, Alam ZM, Shomstein S, Wassermann EM. 2018. Left-shifting prism adaptation boosts reward-based learning. *Cortex*. 109:279–286.

Schintu S, Martín-Arévalo E, Vesia M, Rossetti Y, Salemme R, Pisella L, Farnè A, Reilly KT. 2016. Paired-pulse parietal-motor

stimulation differentially modulates corticospinal excitability across hemispheres when combined with prism adaptation. *Neural Plast*. 2016:1–9.

Schintu S, Pisella L, Jacobs S, Salemme R, Reilly KT, Farnè A. 2014. Prism adaptation in the healthy brain: the shift in line bisection judgments is long lasting and fluctuates. *Neuropsychologia*. 53:165–170.

Schmahmann JD. 2010. The role of the cerebellum in cognition and emotion: personal reflections since 1982 on the dysmetria of thought hypothesis, and its historical evolution from theory to therapy. *Neuropsychol Rev*. 20:236–260.

Schmahmann JD, Sherman JC. 1998. The cerebellar cognitive affective syndrome. *Brain*. 121:561–579.

Silver MA, Kastner S. 2009. Topographic maps in human frontal and parietal cortex. *Trends Cogn Sci*. 13:488–495.

Striemer CL, Danckert JA. 2010. Through a prism darkly: re-evaluating prisms and neglect. *Trends Cogn Sci*. 14:308–316.

Szczepanski SM, Kastner S. 2013. Shifting attentional priorities: control of spatial attention through hemispheric competition. *J Neurosci*. 33:5411–5421.

Talairach P, Tournoux J. 1988. Co-Planar Stereotaxic Atlas of the Human Brain. New York: Thieme.

Tissieres I, Fornari E, Clarke S, Crottaz-Herbette S. 2018. Supramodal effect of rightward prismatic adaptation on spatial representations within the ventral attentional system. *Brain Struct Funct*. 223:1459–1471. doi: 10.1007/s00429-017-1572-2 (last accessed 11 May 2018).

Tsujimoto K, Mizuno K, Nishida D, Tahara M, Yamada E, Shindo S, Kasuga S, Liu M. 2018. Prism wadaptation changes resting-state functional connectivity in the dorsal stream of visual attention networks in healthy adults: A fMRI study. *Cortex*. http://www.sciencedirect.com/science/article/pii/S0010945218303514 (last accessed 7 January 2019).

Vallar G, Bottini G, Rusconi ML, Sterzi R. 1993. Exploring somatosensory hemineglect by vestibular stimulation. *Brain*. 116:71–86.

Ventre-Dominey J, Vighetto A, Denise P. 1999. Vestibulo-ocular dysfunction induced by cortical damage in man: a case report. *Neuropsychologia*. 37:715–721.

Wang L, Mruczek REB, Arcaro MJ, Kastner S. 2015. Probabilistic Maps of Visual Topography in Human Cortex. *Cereb Cortex N Y NY*. 25:3911–3931.

Wang JX, Rogers LM, Gross EZ, Ryals AJ, Dokucu ME, Brandstatt KL, Hermiller MS, Voss JL. 2014. Targeted enhancement of cortical-hippocampal brain networks and associative memory. *Science*. 345:1054–1057.

Watson TC, Obiang P, Torres-Herraez A, Watilliaux A, Coulon P, Rochefort C, Rondi-Reig L. 2019. Anatomical and physiological foundations of cerebello-hippocampal interaction. *elife*. 8:e41896.

Weiner MJ, Hallett M, Funkenstein HH. 1983. Adaptation to lateral displacement of vision in patients with lesions of the central nervous system. *Neurology*. 33:766–766.

Werner S, Schorn CF, Bock O, Theysohn N, Timmann D. 2014. Neural correlates of adaptation to gradual and to sudden visuomotor distortions in humans. *Exp Brain Res*. 232:1145–1156.

Whitlock JR, Sutherland RJ, Witter MP, Moser M-B, Moser EI. 2008. Navigating from hippocampus to parietal cortex. *Proc Natl Acad Sci*. 105:14755–14762.

Wilf M, Serino A, Clarke S, Crottaz-Herbette S. 2019. Prism adaptation enhances decoupling between the default mode network and the attentional networks. *NeuroImage*. 200:210–220.

World Medical Association. 2013. World medical association declaration of Helsinki: ethical principles for medical research involving human subjects. *JAMA*. 310:2191–2194.